Depth-Dependent Spin Dynamics in Thin Films of $TbPc_2$ Nanomagnets Explored by Low-Energy Implanted Muons

Andrea Hofmann,[†] Zaher Salman,[†,*] Matteo Mannini,[‡] Alex Amato,[†] Luigi Malavolti,[‡] Elvezio Morenzoni,[†] Thomas Prokscha,[†] Roberta Sessoli,[‡] and Andreas Suter[†]

[†]Laboratory for Muon Spin Spectroscopy, Paul Scherrer Institute, CH-5232 Villigen PSI, Switzerland, and [‡]Dipartimento di Chimica, Università di Firenze & INSTM, Via della Lastruccia 3, 50019 Sesto Fiorentino, Italy

ABSTRACT We present measurements of the magnetic properties of thin film $TbPc_2$ single-molecule magnets evaporated on a gold substrate and compare them to those in bulk. Zero-field muon spin relaxation measurements were used to determine the molecular spin fluctuation rate of $TbPc_2$ as a function of temperature. At low temperature, we find that the fluctuations in films are much faster than in bulk and depend strongly on the distance between the molecules and the Au substrate. We measure a molecular spin correlation time that varies between 1.4 μs near the substrate and 6.6 μs far away from it. We attribute this behavior to differences in the packing of the magnetic cores, which change gradually on the scale of ~10−20 nm away from the $TbPc_2$/Au interface.

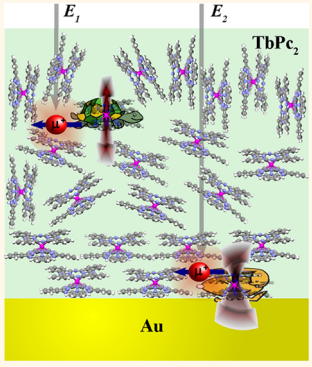

KEYWORDS: single-molecule magnets · $TbPc_2$ · thin films · low-energy muon spin relaxation · quantum tunneling of the magnetization

A promising strategy to encode information in molecular units is provided by single-molecule magnets (SMMs),[1,2] chemically identical nanoscale clusters of exchange-coupled transition metal or rare earth ions and associated ligands. SMMs have been used to study quantum tunneling of magnetization and topological quantum phase interference[3] and may find applications in quantum information processing.[4−6] The assembly of these systems on surfaces is currently investigated,[7−18] as this represents a necessary prerequisite for their technological applications. However, neither the effect of the surface on the magnetic properties of individual SMMs nor that of reduced dimensionality is well understood. One of the most investigated SMMs is $TbPc_2$ ($Tb(C_{32}H_{16}N_8)_2 \cdot CH_2Cl_2$ in bulk), whose chemical robustness enables thermal evaporation on surfaces[19−24] and inclusion in nanogaps, allowing the electronic readout of a single nuclear spin.[25]

As far as the magnetic properties are concerned, the ground spin state manifold, $\mathbf{J} = 6$, of $TbPc_2$ is split by a strong crystal field at the single Tb^{3+} ion, which results in a separation between the ground state, $J_z = \pm 6$, and the first excited state, $J_z = \pm 5$, on the order of a few hundred Kelvin.[26,27] The exceptionally large anisotropy of $TbPc_2$, as well as the long correlation time of its molecular spin fluctuations, makes the system a promising candidate for applications in quantum computation.[28] In the crystalline phase, $TbPc_2$ is characterized by a low-temperature butterfly-shaped hysteresis, which opens at temperatures as high as 15 K. In contrast, submonolayers of $TbPc_2$ on Au(111) do not show a similarly high blocking temperature.[20] Recently, deposition on ferromagnetic substrates revealed an antiferromagnetic interaction with the substrate,[21] most likely mediated by the phthalocyanine (Pc) molecules,[29] but the observed magnetic bistability is reminiscent of that of the substrate. The weak hysteresis in submonolayers on various conducting surfaces may be due to the effects of the substrate on the magnetization dynamics or possibly variation in the intermolecular interactions between neighboring $TbPc_2$. However, the exact details of how and why the low-temperature dynamics are affected are still not clear. Therefore, a better understanding of the phenomenon is mandatory if these types of molecules are to be used in spintronic devices. Here we use the muon spin relaxation (μSR, see Methods) technique to measure the local spin dynamics of $TbPc_2$ and its depth dependence

* Address correspondence to zaher.salman@psi.ch.

Received for review July 16, 2012 and accepted August 23, 2012.

Published online August 23, 2012
10.1021/nn3031673

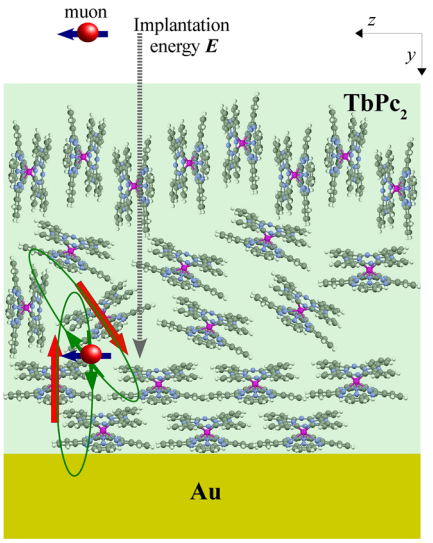

Figure 1. Schematic of a typical LE-μSR experiment. Fully spin-polarized muons (along *z*) are implanted with energy *E* into a thin film of $TbPc_2$ and sense the dipolar magnetic fields from moments of neighboring SMMs. The muon mean implantation depth is proportional to *E*.

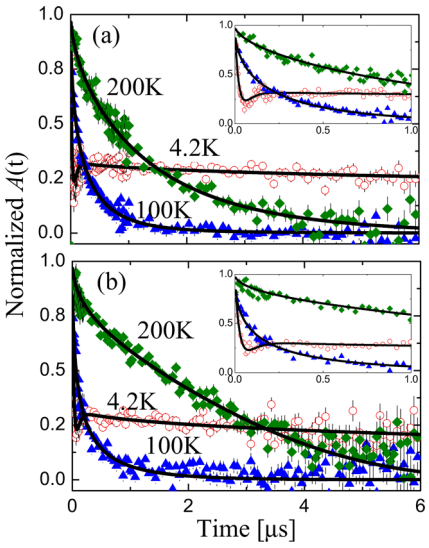

Figure 2. Typical muon spin relaxation curves in the (a) bulk and (b) thick film samples measured in ZF and various temperatures. The insets show the early time relaxation, where the dip in the relaxation can be clearly seen at low temperatures. The lines are fits to eq 1.

in thin films evaporated on a Au surface. In these experiments, fully spin-polarized muons are implanted into the sample and used as a local probe to detect dipolar fields from their neighboring molecules (see Figure 1). Thus, they provide a direct observation of the spin dynamics of individual SMMs. This resolution, coupled with the unique sensitivity to fluctuation times in the range $\sim 10^{-11}$ to 10^{-4} s, makes this technique very suitable for studies of SMMs, both in the bulk and at the nanoscale. We show that the $TbPc_2$ relaxation of the magnetization in films is faster than in bulk crystalline powder. Contrary to what is expected, we conclude that this effect is not substrate induced but is rather related to the packing of the $TbPc_2$ molecules. The reported measurements are a first example of application for Low Energy Muon Spin Relaxation (LE-μSR) in molecular magnetic nanostructures.

RESULTS AND DISCUSSION

In our study we compared zero magnetic field (ZF) μSR measurements performed on three samples of $TbPc_2$: (1) a bulk powder sample and (2) a thick ($\sim 1\ \mu$m) and (3) a thin ($\sim$100 nm) film sample evaporated onto 200 nm polycrystalline gold films grown on freshly cleaved Muscovite mica substrates. The $TbPc_2$ evaporation was performed in ultrahigh vacuum (UHV) using a home-built evaporator, which was heated to 690 K. While in the thin film the whole thickness can be probed by muons, in the thick film the thickness largely exceeds the muons' penetration depth. The thickness of deposit was estimated by atomic force microscopy (AFM) with the standard scratch method and verified by magnetometry measurements.[11]

Example muon spin relaxation curves measured in ZF in the bulk and thick film samples are presented in Figure 2a and b, respectively. The measurements in both samples exhibit a striking qualitative similarity in the whole temperature range. Note that at low temperatures the asymmetry in both samples exhibits a dip at early times (insets of Figure 2), followed by a recovery and then relaxation at longer times. In contrast, at high temperature the asymmetry relaxes in an exponential-like manner from its initial value to zero. The low-temperature relaxation curves, with slowly relaxing tail, indicate that the internal magnetic field experienced by the implanted muons in $TbPc_2$ contains two contributions: a static component and a dynamic component. Here, the terms dynamic and static are relative to the ratio $\nu/(\gamma\delta)$, where ν is the fluctuation rate of the dynamic magnetic fields, $\gamma/2\pi =$ 135.5 MHz/T is the muon's gyromagnetic ratio, and δ is the width of static magnetic field distribution sensed by the muon. The static case is approached when the ratio is $\ll 1$, while the fast fluctuation limit is approached when the ratio is $\gg 1$.

When muons experience a distribution of static magnetic fields with an additional dynamic component, the muon spin relaxation curve can be described by the phenomenological static Kubo–Toyabe function, multiplied by a suitable dynamic relaxation.[30,31] The form of the Kubo–Toyabe function depends on the distribution of static fields sensed by the implanted muons, *e.g.*, Gaussian or Lorentzian. In our case, the asymmetry measured in $TbPc_2$ at all temperatures was found to fit best to a Lorentzian Kubo–Toyabe multiplied by a square root exponential relaxation,

$$A(t) = \frac{A_0}{3}\,[1 + 2(1 - \gamma\delta t)e^{-\gamma\delta t}]e^{-\sqrt{\lambda t}} \qquad (1)$$

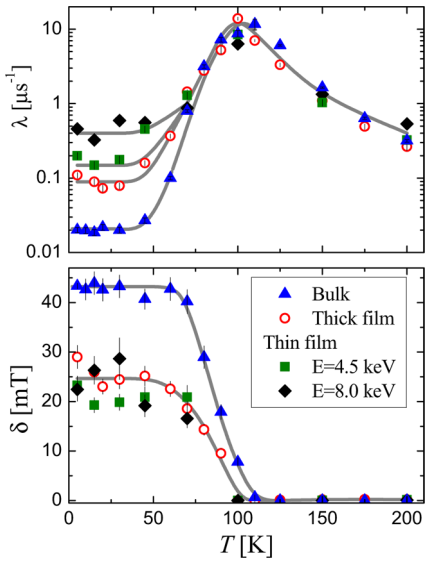

Figure 3. λ (top) and δ (bottom) as a function of temperature in both the bulk and thin film samples obtained from fits of the relaxation curves to eq 1. The lines are a guide to the eye.

where A_0 is the initial asymmetry, γ is the muon's gyromagnetic ratio, δ is the half-width at half-maximum of the static field distribution, and λ is the relaxation rate, containing information regarding the dynamics of the local field. The square root exponential relaxation reflects the averaging of the relaxation behavior of muons stopping in many inequivalent sites.[32−37] The parameters λ and δ obtained from fits to eq 1, which is suitable for describing the data in bulk as well as thin films, are shown in Figure 3. Note that our bulk results are consistent with previous μSR measurements.[37] The qualitative similarity between bulk and thin film behavior is a strong indication that the SMM nature of $TbPc_2$ in the films is maintained. The static and dynamic behavior in all three samples are in fact characterized by three different temperature regimes. At high temperatures λ is small and $\delta \approx 0$. As the temperature is decreased λ increases sharply while δ remains zero. At ~100 K, λ peaks and δ becomes nonzero. Finally, below ~50 K both λ and δ saturate and become temperature independent. However, quantitative differences are observed at low temperature between the bulk and the films; for example, the saturation values of δ are ~42 and ~24 mT in the bulk and film samples, respectively. It is important to point out here that δ is equal in both film samples throughout the whole temperature range and is even independent of the muons' implantation energy, E, which is proportional to the implantation depth. At high temperatures, λ, which is directly related to the spin dynamics, is also equal in both films and is E independent. However, at low temperatures, and only in the thin film, it depends strongly on E.

We consider first the static magnetic field component experienced by muons. At high temperatures, $\delta \approx 0$ reflects the absence of static fields as a consequence

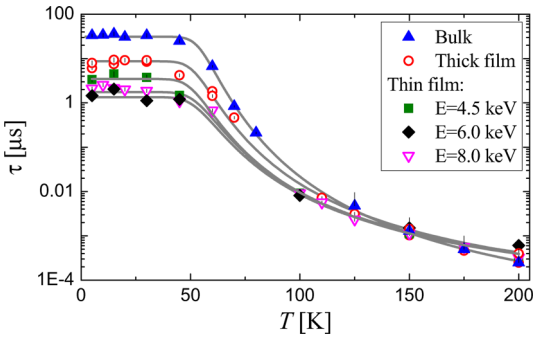

Figure 4. Correlation time as a function of temperature measured in bulk and $TbPc_2$ films. The lines are fits to eq 3.

of fast thermal fluctuations between the ground ($J_z = \pm 6$) and first excited ($J_z = \pm 5$) spin states, whereas the temperature-independent saturation of δ at low temperatures indicates that muons experience a temperature-independent distribution of static fields. In fact, at this temperature we expect all molecules to reside in the ground state, since the energy gap to the next excited state is more than ~650 K (see below).

Information regarding the dynamics of the local field can be extracted from λ. The exponential increase as the temperature is decreased in the high-temperature regime demonstrates the slowing spin dynamics. This is due to the reduced probability of spin-phonon-mediated transitions between different spin states.[33,38,39] The small difference in λ between bulk and films in this temperatures regime implies that the energy gap between the ground and first excited states does not change significantly. This is direct evidence that there is almost no change in the crystal field of the Tb ions between bulk and films. In contrast to this behavior, the saturation of λ at low temperature is a consequence of persistent spin dynamics at temperatures far below the energy gap. This is attributed to quantum tunneling between the two quasi-degenerate $J_z = \pm 6$ ground states,[36,37] which is particularly efficient in zero applied magnetic field, corresponding to the condition of our experiment. Interestingly, in Figure 3 one can observe a clear difference in the saturation value of λ depending on the sample: bulk, thick or thin film. Moreover, in the thin film it also depends on the muons' implantation energy/depth. In what follows we extract the correlation time of the molecular spin dynamics as a function of temperature.

At low temperatures where $\gamma\delta > \lambda$, $A(t)$ is almost identical to the well-known dynamic Lorentzian Kubo−Toyabe function, and hence $\lambda = (2/3\tau)$,[40,32] where τ is the correlation time of the local magnetic field experienced by the muon,[31] which in our case is that generated by the $TbPc_2$ SMM. However, at high temperatures, where $\delta \approx 0$, the relaxation rate can be written as $\lambda = 2\tau(\gamma\delta_0)^2$,[32,40] where δ_0 is the size of the fluctuating field at the measured temperature. Note that the SMMs are in their ground **J** = 6 manifold

TABLE 1. Summary of Parameters from Fits of τ as a Function of T to eq 3

parameter	bulk	thick film (~1 μm)	thin film (~100 nm)
C [$10^{-14}/\mu s \cdot K^3$]	6.2 ± 2.5	1.1 ± 0.2	0.51 ± 0.22
Δ [K]	877 ± 30	790 ± 10	640 ± 30
τ_q [μs]	31.2 ± 1.6	6.6 ± 0.2	see Figure 5

throughout the measured temperature range. Therefore, δ_0 can be evaluated from the low-temperature saturation value, $\delta_0 = \delta(T \rightarrow 0)$, which reflects the size of the dipolar field from the magnetic moment of a single $TbPc_2$ molecule. Thus, we can readily extract τ as a function of temperature in the high- and low-temperature ranges, as shown in Figure 4. The probability (or inverse correlation time) of phonon-induced transitions between the $J_z = \pm 6$ and $J_z = \pm 5$ states is[33,38,39]

$$\frac{1}{\tau_{sp}} = C\Delta^3 \exp\left(\frac{\Delta}{T}\right) \quad (2)$$

where C is a temperature-independent parameter that represents the spin-phonon coupling strength and Δ is the energy gap between the spin states. This accounts for the observed high-temperature dependence of τ, but given the exponential dependence and the large value of Δ, no spin dynamics is expected at low temperatures. However, in the low-temperature regime of our μSR data we find that τ is finite and temperature-independent. In order to model these results, we add a phenomenological constant contribution at low temperatures, τ_q, which reflects the contribution of quantum tunneling between $J_z = \pm 6$ states to the correlation time. Thus, the full probability for transitions between different sublevels of the **J** = 6 manifold is[39]

$$\frac{1}{\tau} = \frac{1}{\tau_q} + \frac{1}{\tau_{sp}} \quad (3)$$

A fit of the μSR results to this model provides the values for Δ, C, and τ_q given in Table 1. We find that Δ is similar in all samples and exhibits no implantation energy dependence, as expected from the similar high-temperature behavior in τ. This confirms that the crystal field experienced by the Tb ions does not depend on sample or depth in the films. The values of C vary significantly between the different samples. This is to be expected between bulk and films, given the reduced/two-dimensional geometry, as well as the loss of solvent molecules in the films.[41] These effects modify the phonon spectrum dramatically and, therefore, affect the value of C. However, the difference between the thick and thin film is surprising, but may also be due to the effect of film thickness on the phonon spectrum when it is decreased from the micrometer to the nanoscale. Most importantly, we note that only in the thin film do we find a clear E/depth dependence of τ_q, as shown in Figure 5. This effect is attributed to a depth-dependent packing of the SMMs as we discuss in more detail below.

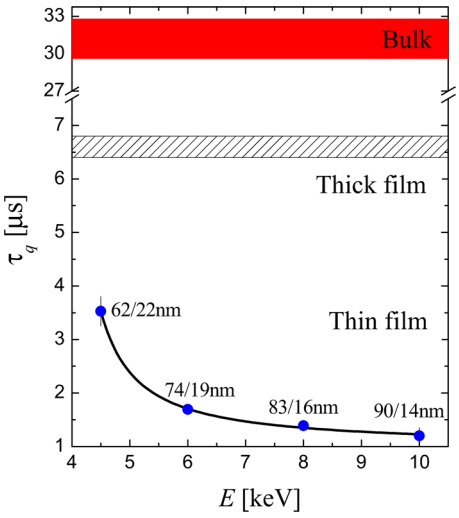

Figure 5. τ_q as a function of E (and corresponding mean/rms implantation depth) obtained from fits of τ as a function of temperature to eq 3. The solid-shaded and hatched areas represent the values (and uncertainty) in the bulk and the thick film samples, respectively.

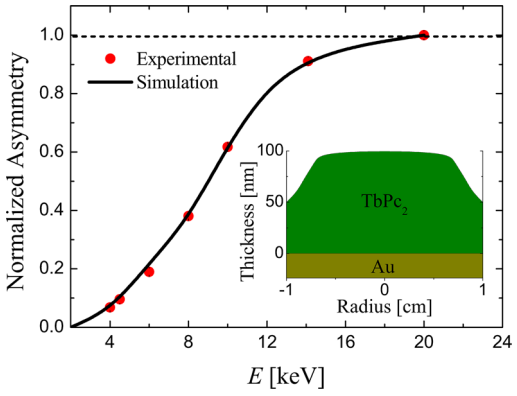

Figure 6. Normalized fraction of muons stopping in the Au substrate as a function of E. The solid line is the estimated value from Trim.SP simulations using a $TbPc_2$ film with a nominal thickness of ~100 nm and a cross-section profile as illustrated in the inset.

To establish a clear relation between the muons' implantation energy and their mean/root mean squared (rms) stopping depth in the $TbPc_2$ film (Figure 5), we use Trim.SP simulations[42] to model experimental measurements. First, we determine the fraction of the asymmetry from muons stopping in the gold substrate as a function of E. For this purpose, we measure $A(t)$ in a magnetic field, B, applied transverse to the initial spin of the muons. At 5 K muons stopping in the $TbPc_2$ film depolarize very rapidly due to the large internal fields, while muons stopping in nonmagnetic gold experience predominantly the applied transverse field and, therefore, precesses at the Larmor frequency, γB. The normalized fraction of precessing signal as a function of E is plotted in Figure 6. Next, we simulate the muon stopping depth profile in a $TbPc_2$ film of density $\rho \approx 1.5 \pm 0.1$ g/cm^3 (Malavolti, L.; *et al.*, unpublished). We further

assume that our muon beam (radius ~1 cm) impinges on a film with thickness cross-section profile as illustrated in the inset of Figure 6, which is suggested by AFM measurements. Best fit to the experimental data is obtained using a film with a nominal thickness of ~100 nm, which falls gradually to ~50 nm at the edges of the beam spot. Note, this method of implantation depth estimate has many potential systematic uncertainties due to the nonuniform thickness profile and density of the film. However, it gives a rough idea of the depth dependence of τ_q as reported in Figure 5. Here, the values of τ_q are essentially a weighted average of the correlation time of the $TbPc_2$ molecules over the full stopping depth distribution of the implanted muons, which provide qualitative information regarding its depth dependence. Interestingly we notice that the depth dependence extends to a scale of 10's nm away from the gold surface. We would like to stress here that this information is accessible thanks to the unique depth sensitivity of the LE-μSR technique.

It is useful to compare our results with recent X-ray magnetic circular dichorism (XMCD) measurements on $TbPc_2$ films[20] and monolayers (ML). These measurements reveal that the magnetic hysteresis in the monolayer deposits disappears.[20] This could be, in principle, associated with an electronic effect induced by the substrate, similar to that observed in phthalocyanine- and porphyrine-based complexes of 3d ions.[43] However, from a comparison between a thin (monolayer) and a thick (~200 nm) film of $TbPc_2$ on Au, it was concluded that the packing of the molecules was different in the two films. In the monolayer, the Pc molecules lie flat on the substrate, resulting in the $TbPc_2$ easy axes pointing out of plane, while in the thick film the molecules are in a standing configuration with an in-plane easy axes. The difference was attributed to a competition between molecule−substrate and molecule−molecule interactions.[44] XMCD is sensitive only to the top few ML, and it does not provide details of the depth dependence of the $TbPc_2$ reorientation. Our μSR measurements complement this picture by revealing a significant depth dependence of the molecular spin dynamics which may be correlated to a gradual variation of the molecular packing. In particular, τ_q is small for high E, *i.e.*, near the interface, and becomes larger as we probe molecules further away from the interface, gradually approaching the value measured in the thick film where all muons stop far from the substrate (few 100's nm away).

The $TbPc_2$ reorientation is not fully unexpected. For simple copper-phthalocyanine (CoPc) complexes, synchrotron-based investigations using near-edge X-ray absorption fine structure spectroscopy and surface-sensitive X-ray photoemission spectroscopy experiments revealed that these flat molecules start to lose their lying orientation on Au(111) substrates after 3 ML and that the standing orientation is fully retrieved after *ca.* 10 ML.[45] In the case of our experiment the relaxation time starts to deviate significantly from that found at the Au interface after *ca.* 30−40 ML. However, without performing measurements on a series of $TbPc_2$ films of different thickness (*e.g.*, using synchrotron-based experiments), it is not possible to determine the length scale of the reorientation process in $TbPc_2$ films (compared to CuPc). Such information can then be correlated with the observed changes in the magnetization dynamics.

A priori, one may suggest that the observed effect on the spin dynamics is due to the different dipolar interactions between the $TbPc_2$ moments as a result of the different packing. Assuming a configuration as revealed by the XMCD results, one can model the distribution of dipolar fields, $p(B)$, on a single molecule from its neighbors at very low temperatures ($T = 0$).[46] Near the $TbPc_2$/Au interface, we assume an ideal case where all spins are arranged (anti)parallel to the normal of the substrate. A key feature of $p(B)$ in this case is that the dipolar field is always pointing along the easy axis of the molecule. Therefore, if sufficiently large, it removes the degeneracy between up and down spin states and prohibits tunneling, thus increasing τ_q (Hofmann, A.; *et al.*, unpublished). Far from the interface, we assume a scenario where all spins are randomly oriented in the plane, which results in a dipolar field distribution that may have parallel as well as perpendicular components to the easy axis of the molecule. Hence, their effect to prohibit tunneling is reduced, and in fact, the perpendicular components may even promote tunneling due to mixing of spin states, leading to a shorter τ_q away from the interface. Note, however, that this model gives contradicting results to our observation. Therefore, we conclude that dipolar fields from neighboring molecules as a result of different packing cannot explain our measurements. We must instead take into account the exchange interactions, mediated by the free electrons on the Pc molecules, which can also affect the magnetization dynamics. Such behavior was observed in cobalt phthalocyanine (CoPc) thin films,[43] which were found to form one-dimensional antiferromagnetic chains in thin films. Similar phenomena were observed in the isostructural YPc_2 molecules, carrying one unpaired electron on the organic shell, which exhibit one-dimensional organic ferromagnetism due to a significant overlap of π orbitals,[41] which depends strongly on the packing of the molecules. In our films, the gradual change in crystal packing moving from the substrate surface toward the top of the molecular film reflects in a gradual change of the magnetization dynamics.

CONCLUSION

We find that the SMM properties of $TbPc_2$ are clearly maintained in thin films. Nevertheless, the molecular spin dynamics are significantly enhanced with proximity of the molecules to the $TbPc_2$/Au substrate

interface. This is consistent with the disappearance of hysteresis in the monolayer observed with XMCD. Thanks to the unique capabilities of the low-energy muon spin relaxation technique in the investigation of magnetic nanostructures, we have however detected a gradual increase of the correlation time from 1.4 ± 0.1 μs near the interface to 6.6 ± 0.2 μs far from it (thick film). This unambiguously proves that other mechanisms, beyond a possible direct interaction with the substrate, are responsible for the disappearance of the hysteresis. It appears to be a characteristic effect of $TbPc_2$ SMMs and their strong sensitivity to their crystalline environment and magnetic dilution (Malavolti, L.; *et al.*, unpublished). A possible explanation is that the depth-dependent packing alters the superexchange interaction between neighboring Pc molecules and in turn the molecular spin dynamics. However, further experiments on isotropic or diamagnetic MPc_2 derivatives are necessary to characterize weak intermolecular interactions. We also find that the correlation time measured in films is much shorter than in the bulk, 31.2 ± 1.6 μs. Nevertheless, the time range of a few μs makes the $TbPc_2$ system a possible candidate for applications in quantum computation even in thin films. Finally, these measurements provide an interesting possibility of controlling the spin dynamics of SMMs by controlling their packing, *e.g.*, by a different choice of substrate or different deposition conditions. This may prove useful for tuning the correlation time of SMMs to match it with a specific potential application.

METHODS

In μSR experiments 100% polarized (along z) positive muons are implanted in the sample. Each implanted muon decays (lifetime $\tau_\mu = 2.2$ μs) emitting a positron preferentially in the direction of the muon polarization at the time of decay. Using appropriately positioned detectors, one measures the asymmetry of the muon decay along z as a function of time, $A(t)$, which is proportional to the time evolution of the muon spin polarization. $A(t)$ depends on the distribution of internal magnetic fields and their temporal fluctuations. Further details on the μSR technique may be found in ref 47. In contrast to conventional bulk μSR, in low-energy μSR (LE-μSR) experiments, the muons' implantation energy (E) can be varied between 1 and 32 keV, corresponding to a typical average implantation depth of 5 to 300 nm, allowing depth-resolved measurements in thin films[48,49] (see Figure 1). The μSR measurements on the bulk sample were performed on the GPS spectrometer, while the thin film measurements were performed on the LE-μSR[48,49] spectrometer, both at the Paul Scherrer Institute in Switzerland.

Conflict of Interest: The authors declare no competing financial interest.

Acknowledgment. This work is based on experiments performed at the Swiss muon source SμS, Paul Scherrer Institute, Villigen, Switzerland. Part of this work has been supported by the ERC Advanced Grant MolNanoMaS (proj. no. 267746) and by Italian MIUR through PRIN "Record" (20097X44S7) and FIRB "NanoPlasMag" (RBFR10OAI0) projects.

REFERENCES AND NOTES

1. Wernsdorfer, W.; Aliaga-Alcalde, N.; Hendrickson, D. N.; Christou, G. Exchange-Biased Quantum Tunnelling in a Supramolecular Dimer of Single-Molecule Magnets. *Nature* **2002**, *416*, 406–409.
2. Gatteschi, D.; Sessoli, R. Quantum Tunneling of Magnetization and Related Phenomena in Molecular Materials. *Angew. Chem., Int. Ed.* **2003**, *42*, 268–297.
3. Wernsdorfer, W.; Sessoli, R. Quantum Phase Interference and Parity Effects in Magnetic Molecular Clusters. *Science* **1999**, *284*, 133–135.
4. Leuenberger, M. N.; Loss, D. Quantum Computing in Molecular Magnets. *Nature* **2001**, *410*, 789–793.
5. Tejada, J.; Chudnovsky, E. M.; del Barco, E.; Hernandez, J. M.; Spiller, T. P. Magnetic Qubits as Hardware for Quantum Computers. *Nanotechnology* **2001**, *12*, 181–186.
6. Ardavan, A.; Rival, O.; Morton, J. J. L.; Blundell, S. J.; Tyryshkin, A. M.; Timco, G. A.; Winpenny, R. E. P. Will Spin-Relaxation Times in Molecular Magnets Permit Quantum Information Processing? *Phys. Rev. Lett.* **2007**, *98*, 057201.
7. Cornia, A.; Mannini, M.; Sainctavit, Ph.; Sessoli, R. Chemical Strategies and Characterization Tools for the Organization of Single Molecule Magnets on Surfaces. *Chem. Soc. Rev.* **2011**, *40*, 3076–3091.
8. Gómez-Segura, J.; Díez-Pérez, I.; Ishikawa, N.; Nakano, M.; Veciana, J.; Ruiz-Molina, D. 2-D Self-Assembly of the Bis-(Phthalocyaninato)Terbium(iii) Single-Molecule Magnet Studied by Scanning Tunnelling Microscopy. *Chem. Commun.* **2006**, 2866–2868.
9. Burgert, M.; Voss, S.; Herr, S.; Fonin, M.; Groth, U.; Rudiger, U. Single-Molecule Magnets: A New Approach to Investigate the Electronic Structure of Mn_{12} Molecules by Scanning Tunneling Spectroscopy. *J. Am. Chem. Soc.* **2007**, *129*, 14362–14366.
10. Moroni, R.; Buzio, R.; Chincarini, A.; Valbusa, U.; de Mongeot, F. B.; Bogani, L.; Caneschi, A.; Sessoli, R.; Cavigli, L.; Gurioli, M. Optically Addressable Single Molecule Magnet Behaviour of Vacuum-Sprayed Ultrathin Films. *J. Mater. Chem.* **2008**, *18*, 109–115.
11. Margheriti, L.; Mannini, M.; Sorace, L.; Gorini, L.; Gatteschi, D.; Caneschi, A.; Chiappe, D.; Moroni, R.; de Mongeot, F. B.; Cornia, A.; *et al.* Thermal Deposition of Intact Tetrairon(III) Single-Molecule Magnets in High-Vacuum Conditions. *Small* **2009**, *5*, 1460–1466.
12. Mannini, M.; Pineider, F.; Sainctavit, P.; Danieli, C.; Otero, E.; Sciancalepore, C.; Talarico, A. M.; Arrio, M.; Cornia, A.; Gatteschi, D; *et al.* Magnetic Memory of a Single-Molecule Quantum Magnet Wired to a Gold Surface. *Nat. Mater.* **2009**, *8*, 194–197.
13. Cavallini, M.; Facchini, M.; Albonetti, C.; Biscarini, F. Single Molecule Magnets: from Thin Films to Nano-Patterns. *Phys. Chem. Chem. Phys.* **2008**, *10*, 784–793.
14. Cornia, A.; Fabretti, A. C.; Pacchioni, M.; Zobbi, L.; Bonacchi, D.; Caneschi, A.; Gatteschi, D.; Biagi, R.; Pennino, U. D.; de Renzi, V; *et al.* Direct Observation of Single-Molecule Magnets Organized on Gold Surfaces. *Angew. Chem., Int. Ed.* **2003**, *42*, 1645–1648.
15. Condorelli, G. G.; Motta, A.; Fragalà, I. L.; Giannazzo, F.; Raineri, V.; Caneschi, A.; Gatteschi, D. Anchoring Molecular Magnets on the Si(100) Surface. *Angew. Chem., Int. Ed.* **2004**, *43*, 4081–4084.
16. Coronado, E.; Forment-Aliaga, A.; Romero, F. M.; Corradini, V.; Biagi, R.; Renzi, V. D.; Gambardella, A.; del Pennino, U. Isolated Mn_{12} Single-Molecule Magnets Grafted on Gold Surfaces *via* Electrostatic Interactions. *Inorg. Chem.* **2005**, *44*, 7693–7695.
17. Fleury, B.; Catala, L.; Huc, V.; David, C.; Zhong, W. Z.; Jegou, P.; Baraton, L.; Palacin, S.; Albouy, P.-A.; Mallah, T. A. New Approach to Grafting a Monolayer of Oriented Mn_{12} Nanomagnets on Silicon. *Chem. Commun.* **2005**, 2020–2022.

18. Salman, Z.; Chow, K. H.; Miller, R. I.; Morello, A.; Parolin, T. J.; Hossain, M. D.; Keeler, T. A.; MacFarlane, W. A.; Saadaoui, H.; Wang, D.; *et al*. Local Magnetic Properties of a Monolayer of Mn_{12} Single Molecule Magnets. *Nano Lett.* **2007**, *7*, 1551–1555.
19. Vitali, L.; Fabris, S.; Conte, A. M.; Brink, S.; Ruben, M.; Baroni, S.; Kern, K. Electronic Structure of Surface-Supported Bis-(Phthalocyaninato) Terbium(III) Single Molecular Magnets. *Nano Lett.* **2008**, *8*, 3364–3368.
20. Margheriti, L.; Chiappe, D.; Mannini, M.; Car, P.; Sainctavit, P.; Arrio, M.; de Mongeot, F. B.; Cezar, J. C.; Piras, F. M.; Magnani, A.; *et al*. X-Ray Detected Magnetic Hysteresis of Thermally Evaporated Terbium Double-Decker Oriented Films. *Adv. Mater.* **2010**, *22*, 5488–5493.
21. Lodi Rizzini, A.; Krull, C.; Balashov, T.; Kavich, J. J.; Mugarza, A.; Miedema, P. S.; Thakur, P. K.; Sessi, V.; Klyatskaya, S.; Ruben, M.; *et al*. Coupling Single Molecule Magnets to Ferromagnetic Substrates. *Phys. Rev. Lett.* **2011**, *107*, 177205.
22. Komeda, T.; Isshiki, H.; Liu, J.; Zhang, Y.; Lorente, N.; Katoh, K.; Breedlove, B. K.; Yamashita, M. Observation and Electric Current Control of a Local Spin in a Single-Molecule Magnet. *Nat. Commun.* **2011**, *2*, 217.
23. Urdampilleta, M.; Klyatskaya, S.; Cleuziou, J.; Ruben, M.; Wernsdorfer, W. Supramolecular Spin Valves. *Nat. Mater.* **2011**, *10*, 502–506.
24. Katoh, K.; Yoshida, Y.; Yamashita, M.; Miyasaka, H.; Breedlove, B. K.; Kajiwara, T.; Takaishi, S.; Ishikawa, N.; Isshiki, H.; Zhang, Y. F.; *et al*. Direct Observation of Lanthanide(III)-Phthalocyanine Molecules on Au(111) by Using Scanning Tunneling Microscopy and Scanning Tunneling Spectroscopy and Thin-Film Field-Effect Transistor Properties of Tb(III)- and Dy(III)-Phthalocyanine Molecules. *J. Am. Chem. Soc.* **2009**, *131*, 9967–9976.
25. Vincent, R.; Klyatskaya, S.; Ruben, M.; Wernsdorfer, W.; Balestro, F. Electronic Read-Out of a Single Nuclear Spin Using a Molecular Spin Transistor. *Nature* **2012**, *488*, 357–360.
26. Ishikawa, N.; Sugita, M.; Ishikawa, T.; Koshihara, S.-y.; Kaizu, Y. Lanthanide Double-Decker Complexes Functioning as Magnets at the Single-Molecular Level. *J. Am. Chem. Soc.* **2003**, *125*, 8694–8695.
27. Takamatsu, S.; Ishikawa, T.; Koshihara, S.-y.; Ishikawa, N. Significant Increase of the Barrier Energy for Magnetization Reversal of a Single-4f-Ionic Single-Molecule Magnet by a Longitudinal Contraction of the Coordination Space. *Inorg. Chem.* **2007**, *46*, 7250–7252.
28. Di Vincenzo, D. P. The Physical Implementation of Quantum Computation. *Fortschr. Phys.* **2000**, *48*, 771–783.
29. Schwöbel, J.; Fu, Y.; Brede, J.; Dilullo, A.; Hoffmann, G.; Klyatskaya, S.; Ruben, M.; Wiesendanger, R. Real-Space Observation of Spin-Split Molecular Orbitals of Adsorbed Single-Molecule Magnets. *Nat. Commun.* **2012**, *3*, 953.
30. Fudamoto, Y.; Gat, I. M.; Larkin, M. I.; Merrin, J.; Nachumi, B.; Savici, A. T.; Uemura, Y. J.; Luke, G. M.; Kojima, K. M.; Hase, M.; *et al*. Muon Spin Relaxation in the Spin-Ring System Cu_3WO_6: Quasistatic Spin Freezing at 7.0 K. *Phys. Rev. B* **2002**, *65*, 174428.
31. Salman, Z.; Giblin, S. R.; Lan, Y.; Powell, A. K.; Scheuermann, R.; Tingle, R.; Sessoli, R. Probing the Magnetic Ground State of the Molecular Dysprosium Triangle with Muon Spin Relaxation. *Phys. Rev. B* **2010**, *82*, 174427.
32. Uemura, Y. J.; Yamazaki, T.; Harshman, D. R.; Senba, M.; Ansaldo, E. J. Muon-Spin Relaxation in AuFe and CuMn Spin Glasses. *Phys. Rev. B* **1985**, *31*, 546–563.
33. Lascialfari, A.; Jang, Z. H.; Borsa, F.; Carretta, P.; Gatteschi, D. Thermal Fluctuations in the Magnetic Ground State of the Molecular Cluster $Mn_{12}O_{12}$ Acetate from μSR and Proton NMR Relaxation. *Phys. Rev. Lett.* **1998**, *81*, 3773–3776.
34. Salman, Z.; Keren, A.; Mendels, P.; Marvaud, V.; Scuiller, A.; Verdaguer, M.; Lord, J. S.; Baines, C. Dynamics at $T \rightarrow 0$ in the Half-Integer Isotropic High Spin Molecules. *Phys. Rev. B* **2002**, *65*, 132403.
35. Blundell, S. J.; Pratt, F. L.; Lancaster, T.; Marshall, I. M.; Steer, C. A.; Heath, S. L.; Letard, J. F.; Sugano, T.; Mihailovic, D.; Omerzu, A. μSR Studies of Organic and Molecular Magnets. *Polyhedron* **2003**, *22*, 1973–1980.
36. Branzoli, F.; Filibian, M.; Carretta, P.; Klyatskaya, S.; Ruben, M. Spin Dynamics in the Neutral Rare-Earth Single-Molecule Magnets $[TbPc_2]^0$ and $[DyPc_2]^0$ from μSR and NMR Spectroscopies. *Phys. Rev. B* **2009**, *79*, 220404.
37. Branzoli, F.; Carretta, P.; Filibian, M.; Graf, M. J.; Klyatskaya, S.; Ruben, M.; Coneri, F.; Dhakal, P. Spin and Charge Dynamics in $[TbPc_2]^0$ and $[DyPc_2]^0$ Single-Molecule Magnets. *Phys. Rev. B* **2010**, *82*, 134401.
38. Villain, J.; Hartman-Boutron, F.; Sessoli, R.; Rettori, A. Magnetic Relaxation in Big Magnetic Molecules. *Europhys. Lett.* **1994**, *27*, 159–164.
39. Salman, Z. Theoretical T_1 Calculation for Isotropic High Spin Molecules. *cond-mat/0209497* **2002**.
40. Hayano, R. S.; Uemura, Y. J.; Imazato, J.; Nishida, N.; Yamazaki, T.; Kubo, R. Zero-and Low-Field Spin Relaxation Studied by Positive Muons. *Phys. Rev. B* **1979**, *20*, 850–859.
41. Paillaud, J. L.; Drillon, M.; De Cian, A.; Fischer, J.; Weiss, R.; Villeneuve, G. Radical-Based Ferromagnetic Chain in Yttrium Diphthalocyanine $[YPc_2]\cdot CH_2Cl_2$. *Phys. Rev. Lett.* **1991**, *67*, 244–247.
42. Eckstein, W. *Computer Simulation of Ion-Solid Interactions*; Springer: Berlin, 1991.
43. Chen, X.; Fu, Y.; Ji, S.; Zhang, T.; Cheng, P.; Ma, X.; Zou, X.; Duan, W.; Jia, J.; Xue, Q. Probing Superexchange Interaction in Molecular Magnets by Spin-Flip Spectroscopy and Microscopy. *Phys. Rev. Lett.* **2008**, *101*, 197208.
44. Biswas, I.; Peisert, H.; Casu, M. B.; Schuster, B.; Nagel, P.; Merz, M.; Schuppler, S.; Chassé, T. Initial Molecular Orientation of Phthalocyanines on Oxide Substrates. *Phys. Status Solidi A* **2009**, *206*, 2524–2528.
45. Biswas, I.; Peisert, H.; Nagel, M.; Casu, M. B.; Schuppler, S.; Nagel, P.; Pellegrin, E.; Chassé, T. Buried Interfacial Layer of Highly Oriented Molecules in Copper Phthalocyanine Thin Films on Polycrystalline Gold. *J. Chem. Phys.* **2007**, *126*, 174704.
46. Vergnani, L.; Barra, A.; Neugebauer, P.; Rodriguez-Douton, M. J.; Sessoli, R.; Sorace, L.; Wernsdorfer, W.; Cornia, A. Magnetic Bistability of Isolated Giant-Spin Centers in a Diamagnetic Crystalline Matrix. *Chem.—Eur. J.* **2012**, *18*, 3390–3398.
47. Yaouanc, A.; de Réotier, P. D. *Muon Spin Rotation, Relaxation, and Resonance: Applications to Condensed Matter*; OUP: Oxford, 2010.
48. Morenzoni, E.; Prokscha, T.; Suter, A.; Luetkens, H.; Khasanov, R. Nano-Scale Thin Film Investigations with Slow Polarized Muons. *J. Phys.: Condens. Matter* **2004**, *16*, S4583–S4601.
49. Prokscha, T.; Morenzoni, E.; Deiters, K.; Foroughi, F.; George, D.; Kobler, R.; Suter, A.; Vrankovic, V. The new μE4 beam at PSI: A Hybrid-Type Large Acceptance Channel for the Generation of a High Intensity Surface-Muon Beam. *Nucl. Instrum. Methods A* **2008**, *595*, 317–331.